

VORTICES IN BOSE–EINSTEIN CONDENSATES: SOME RECENT DEVELOPMENTS

P. G. KEVREKIDIS

*Department of Mathematics and Statistics,
University of Massachusetts, Amherst, MA 01003, USA
kevrekid@math.umass.edu*

R. CARRETERO-GONZÁLEZ

Nonlinear Dynamical Systems Group,
Department of Mathematics and Statistics,
San Diego State University, San Diego, CA 92182-7720, USA
<http://www.rohan.sdsu.edu/~rcarrete>*

D. J. FRANTZESKAKIS

*Department of Physics, University of Athens,
Panepistimiopolis, Zografos, Athens 15784, Greece
dfrantz@cc.uoa.gr*

I. G. KEVREKIDIS

*Department of Chemical Engineering and PACM, Princeton University,
6 Olden Str. Princeton, NJ 08544, USA
yannis@princeton.edu*

Received 16 November 2004

In this brief review we summarize a number of recent developments in the study of vortices in Bose–Einstein condensates, a topic of considerable theoretical and experimental interest in the past few years. We examine the generation of vortices by means of phase imprinting, as well as via dynamical instabilities. Their stability is subsequently examined in the presence of purely magnetic trapping, and in the combined presence of magnetic and optical trapping. We then study pairs of vortices and their interactions, illustrating a reduced description in terms of ordinary differential equations for the vortex centers. In the realm of two vortices we also consider the existence of stable dipole clusters for two-component condensates. Last but not least, we discuss mesoscopic patterns formed by vortices, the so-called vortex lattices and analyze some of their intriguing dynamical features. A number of interesting future directions are highlighted.

Keywords: Bose–Einstein condensation; vortices; existence; stability; dynamics; matter waves; vortex dipoles; vortex lattices.

*URL: <http://nlds.sdsu.edu/>

1. Abbreviations

- BEC: Bose–Einstein condensate
- GP: Gross–Pitaevskii (Equation)
- MD: Molecular dynamics
- MT: Magnetic trap
- OL: Optical lattice
- PR: Parrinello–Rahman
- TF: Thomas–Fermi
- NLS: Nonlinear Schrödinger (Equation)

2. Overview

Bose–Einstein condensation (BEC) was theoretically predicted by Bose and Einstein in 1924.^{1–3,a} It consists of the macroscopic occupation of the ground state of a gas of bosons, below a critical transition temperature T_c , i.e. a quantum phase transition. However, this prediction was only experimentally verified after 70 years, by an amazing series of experiments in 1995 in dilute atomic vapors, namely of rubidium⁴ and sodium.⁵ In the same year, first signatures of the occurrence of BECs were also reported in vapors of lithium⁶ (and were later more systematically confirmed). The ability to controllably cool alkali atoms (currently over 35 groups around the world can routinely produce BECs) at sufficiently low temperatures and confine them via a combination of magnetic and optical techniques (for a review see Ref. 7), has been instrumental in this major feat whose significance has already been acknowledged through the 2001 Nobel prize in Physics.

This development is of particular interest also from a theoretical/mathematical standpoint. On the one hand, there is a detailed experimental control over the produced BECs. On the other, equally importantly, there is a very good model partial differential equation (PDE) that can describe, at the mean-field level, the behavior of the condensates. This model (which, at heart, approximates a quantum many-body interaction with a classical, but nonlinear self-interaction) is the well known Gross–Pitaevskii equation,^{8,9} a variant of the famous Nonlinear Schrödinger equation (NLS)¹⁰ that reads:

$$i\hbar\Psi_t = -\frac{\hbar^2}{2m}\Delta\Psi + g|\Psi|^2\Psi + V_{\text{ext}}(\mathbf{r})\Psi, \quad (1)$$

where Ψ is the mean-field condensate wavefunction (the atom density is $n = |\Psi(x, t)|^2$), Δ is the Laplacian, m is the atomic mass, and the nonlinearity coefficient g (arising from the interatomic interactions) is proportional to the atomic scattering length.⁷ This coefficient is positive (e.g. for rubidium and sodium) or negative (e.g. for lithium) for repulsive or attractive interatomic interactions respectively, corresponding to defocusing or focusing cubic (Kerr) nonlinearities in the context of nonlinear optics.¹⁰ Notice, however, that experimental “wizardry” can even manipulate the scattering length (and thus, the nonlinearity coefficient g) using the so-called Feshbach resonances¹¹ to achieve any positive or negative

^aWe should mention that part of this overview section has significant overlap with the earlier review of two of the present authors on “Pattern Forming Dynamical Instabilities of Bose–Einstein Condensates” (Ref. 51 herein); it is included, however, here for reasons of completeness.

value of the scattering length at will [i.e. nonlinearity strength in Eq. (1)]. Moreover, the external potential V_{ext} can assume different forms. For the “standard” magnetic trap (MT) usually implemented to confine the condensate, this potential has a typical harmonic form:

$$V_{\text{MT}} = \frac{1}{2}m(\omega_x^2 x^2 + \omega_y^2 y^2 + \omega_z^2 z^2), \quad (2)$$

where, in general, the trap frequencies $\omega_x, \omega_y, \omega_z$ along the three directions are different. As a result, in recent experiments, the shape of the trap (and hence, the form of the condensate itself) can range from isotropic to the so-called cigar-shaped traps (see example Ref. 7), to quasi-two-dimensional,¹² or even quasi-one-dimensional forms.¹³ Moreover, linear ramps of (gravitational) potential $V_{\text{ext}} = mgz$ have also been experimentally used.¹⁴ Another prominent example of an experimentally feasible potential is imposed by a pair of laser beams forming a standing wave which generates a periodic optical potential, the so-called optical lattice (OL),^{15–18} of the form:

$$V_{\text{OL}} = V_0 \left[\cos^2 \left(\frac{2\pi x}{\lambda_x} + \phi_x \right) + \cos^2 \left(\frac{2\pi y}{\lambda_y} + \phi_y \right) + \cos^2 \left(\frac{2\pi z}{\lambda_z} + \phi_z \right) \right], \quad (3)$$

where $\lambda_{x,y,z} = \lambda_{\text{laser}} \sin(\theta_{x,y,z}/2)/2$, in which λ_{laser} is the laser wavelength, θ is the angle between the laser beams,¹⁹ and $\phi_{x,y,z}$ is a phase detuning factor (both the latter are potentially variable). Such potentials have been realized in one,^{15,16} two (the so-called egg-carton potential)²⁰ and three dimensions.^{12,21}

Moreover, present experimental realizations render feasible/controllable the adiabatic or abrupt displacement of the magnetic or optical lattice trap^{19,22,23} (inducing motion of the condensates), the “stirring” of the condensates providing angular momentum and creating excitations with topological charge such as vortices^{24–26} and vortex lattices thereof.^{27–29} Additionally, phase engineering of the condensates is also feasible experimentally,³⁰ and this technique has been used in order to produce nonlinear matter-waves, such as dark solitons^{31,32} in repulsive BECs. Note that more recently, bright solitons have been generated as well^{33,34} in attractive BECs, and both types are currently being studied extensively.

Among these coherent structures, of particular interest are the nonlinear waves of nonvanishing vorticity. Vortices are worth studying not only due to their significance as a fundamental type of coherent nonlinear excitations but also because they play a dominant role in the breakdown of superflow in Bose fluids.^{35–37} The theoretical description of vortices in BECs can be carried out in a much more efficient way than in liquid He (see Ref. 38) due to the weakness of the interactions in the former case. These advantages explain a large volume of work regarding the behavior of vortices in BECs, some of which have been summarized in Ref. 39. It is interesting to note in this connection that the description of such topologically charged nonlinear waves and their surprisingly ordered and robust lattices, as well as their role in phenomena as rich and profound as superconductivity and

superfluidity were connected to the theme of the recent Nobel prize in Physics in 2003.

It is around this exciting frontier of theoretical and experimental studies between atomic physics, soft condensed matter physics and nonlinear dynamics that this brief review is going to revolve. Our aim is to report some recent developments in the study of vortices in the context of mean-field theory (i.e. employing the GP equation). We consider various external potentials relevant to the trapping of the condensates, examining the existence, generation and dynamical stability of such coherent structures. It should be noted, however, that all the perturbations considered herein will preserve the Hamiltonian structure of the system. We will discuss these notions at various levels of increasing complexity, starting from that of a single vortex (in Sec. 3), proceeding to that of a few vortices and using the two-vortex system as a characteristic example (in Sec. 4), while in Sec. 5, we will address the behavior of large clusters of vortices, the so-called vortex lattices. Section 6 summarizes our findings and presents some interesting directions for future studies.

3. Single Vortex

3.1. Generation

It is well known that if a superfluid is subjected to rotational motion, vortices will be generated in it. Such a situation also occurs in dilute BECs, where quantized vortices can be described in the framework of the GP equation. Thus, in this context, a vortex can typically be created upon “stirring” the condensate. In particular, beyond a critical angular velocity Ω_c , the energy functional associated with the GP equation (incorporating the centrifugal term due to rotation), namely

$$E = \int d\mathbf{r} \left[-\frac{1}{2}\Psi^* \Delta \Psi + V_{\text{ext}}|\Psi|^2 + \frac{g}{2}|\Psi|^4 - \Omega_z \Psi^* L_z \Psi \right], \quad (4)$$

is minimized by a single vortex configuration,⁴⁰ resulting in the generation of such a structure, observed also experimentally.²⁵ Note that in Eq. (4), $\Omega_z > \Omega_c$ is the angular velocity and $L_z = i(x\partial_y - y\partial_x)$ represents the angular momentum along the z -axis (\star stands for complex conjugate).

However, vortices can be spontaneously produced in a number of alternative ways, some of which we examine in what follows. More specifically:

- (1) they can *spontaneously emerge* as the pattern forming outcome of *dynamical instabilities*, or
- (2) they may be *imprinted* on the condensate via appropriate modulation of its *phase*.

One instability that can be exploited as a method of producing vortex patterns is the so-called transverse or (“snaking”) instability of *rectilinear* dark solitons. This instability, which has been studied extensively in the context of nonlinear optics

(see examples Refs. 41 and 42 for a review), forces a dark soliton to undergo transverse modulations that cause the nodal plane to decay into vortex pairs. The snake instability is known to occur in trapped BECs as well (see Ref. 32 for its experimental observation and Ref. 43 for relevant analytical and numerical results). In this context, dark solitons are placed on top of an inhomogeneous background, the so-called Thomas–Fermi (TF) cloud, which approximately yields the ground state wavefunction in the case of repulsive condensates ($g > 0$),⁷ and can be expressed as

$$\Psi_{\text{TF}} = \exp(-i\mu t) \sqrt{\frac{\max\{\mu - V_{\text{ext}}, 0\}}{g}}, \tag{5}$$

where μ is the condensate’s chemical potential. The snake instability of dark solitons in trapped BECs sets in whenever the soliton motion is subject to a strong coupling between the longitudinal and transverse degrees of freedom, i.e. far from 1D geometries. A relevant discussion demonstrating how the snaking instability manifests itself as the transverse confinement becomes weak, giving rise to the formation of vortices can be found in the recent work of Ref. 44.

To quantify better the above, we follow Ref. 45 to analyze the transverse instability via length-scale competition arguments. In particular, we first consider the following dimensionless 2D version (relevant for a quasi-two-dimensional, or “pancake” BEC lying on the $x - y$ plane) of the original GP equation,

$$i\Psi_t = -\frac{1}{2}\Delta_{\perp}\Psi + |\Psi|^2\Psi + V_{\text{ext}}(r)\Psi, \tag{6}$$

in which length is scaled in units of the fluid healing length $\xi = \hbar/\sqrt{n_0 g m}$ (n_0 is the peak density of the gas in the radial direction), t in units of ξ/c (where $c = \sqrt{n_0 g/m}$ is the Bogoliubov speed of sound), and the atomic density is rescaled by the peak density n_0 ; finally, the external potential is $V_{\text{ext}}(r) = (1/2)\Omega^2 r^2$, where $r^2 = x^2 + y^2$ and the parameter $\Omega = \sqrt{\omega_{\perp}/\omega_z}(4\pi a l_{\perp} n_0)^{-1}$ (where $l_{\perp} = \sqrt{\hbar/m\omega_{\perp}}$ is the transverse harmonic oscillator length, ω_{\perp} being the transverse confining frequency) express the dimensionless effective magnetic trap strength. In the context of Eq. (6), and in the absence of the potential, the transverse instability occurs for perturbation wavenumbers

$$k < k_{\text{cr}} \equiv \left\{ 2\sqrt{\sin^4 \phi + \cos^2 \phi} - [1 + \sin^2(\phi)] \right\}^{1/2}, \tag{7}$$

where $\cos \phi$ is the dark-soliton amplitude (depth) and $\sin \phi$ is its velocity.⁴¹ In the case of stationary (black) solitons $\cos \phi = 1$, hence $k_{\text{cr}} = 1$. On the other hand, in the presence of the potential, the characteristic length scale of the BEC (i.e. the diameter of the cloud in the TF approximation) is $R_{\text{BEC}} = 2^{3/2}\mu_0^{1/2}/\Omega$, where μ_0 is the dimensionless chemical potential. Then, one can argue that the criterion for the suppression of the transverse instability is that the scale of the BEC be shorter than

the minimal one necessary for the onset of the instability, leading to the condition

$$\Omega > \frac{\sqrt{2\mu_0}}{\pi}. \quad (8)$$

If inequality (8) is not satisfied, the transverse instability should develop, resulting in the breakup of the dipole configurations (resulting from a dark soliton, truncated by the Thomas–Fermi state) into vortex–antivortex pairs. It is relevant to note that similar to the case of rectilinear solitons, the snake instability of the *ring* dark solitons can also be responsible for the creation of vortices and vortex arrays as well. In particular, as far as the ring dark solitons are concerned, they were previously predicted in the context of nonlinear optics,⁴⁶ where their properties were studied both theoretically⁴⁷ and experimentally.⁴⁸ These entities were also found to exist in the context of BECs⁴⁹ (see also the relevant recent work⁵⁰). In the latter context, and in the case of sufficiently large initial soliton amplitudes, ring dark solitons were observed to be dynamically unstable towards azimuthal perturbations that led to (snaking and) their breakup into vortex–antivortex pairs, as well as robust vortex arrays, the so-called “vortex necklaces”. The latter consist of four vortex-pair patterns, with their shape alternating between an “X” and a cross (for details, see Figs. 3 and 4 of Ref. 49). We do not discuss these instabilities further, as they were analyzed in some detail in the recent review of Ref. 51.

A context similar to that of pattern forming instabilities, and one which may be loosely related to the Landau instability of superflows, involves the interaction of the condensate with an impurity in a recently proposed dynamical experiment⁵² (which bears resemblances to the phenomenon of vortex trailing in fluids, see e.g. Ref. 53). In particular, in Ref. 52 [and in the framework of the dimensionless GP Eq. (6)], the magnetic trap originally trapping the condensate at $(0, 0)$, was proposed to be displaced by a displacement of x_0 , but also in the presence of an additional anisotropic impurity potential of the form $V_{\text{imp}} = V_0 \text{sech}^2(\sqrt{(x/r_x)^2 + (y/r_y)^2})$ with $V_0 = 0.5$, $r_y = 10$ and $r_x = 5$. If the displacement (which was giving rise to an oscillating motion of the condensate) was subcritical, then it was observed that it did not lead to the formation of “coherent structure radiation.” For supercritical displacements, it was observed to give rise to the formation of vortex pairs, as shown in the results of Fig. 1. The critical speed (proportional to the critical displacement) acquired by the condensate upon “impact” with the impurity was numerically observed in Ref. 52 to closely match an effective speed of sound in the inhomogeneous medium (i.e. in the presence of the parabolic potential), indicating the possibility to attribute the vortex production in this context to a Landau-type instability.^{54,55}

Let us conclude this section by briefly discussing one of the standard techniques that have been implemented to create dark solitons and vortices in trapped BECs, namely the so-called phase imprinting or phase engineering technique. According to the latter, a dark soliton can be generated upon imprinting a phase difference of π along the condensate.^{30–32} On the other hand, in the case of vortices, imprinting

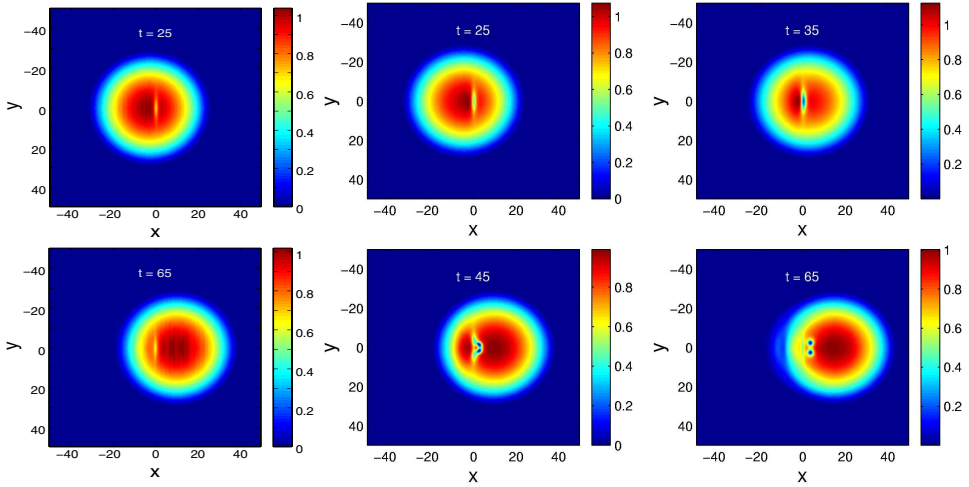


Fig. 1. Comparison of a subcritical case for $x_0 = 10$ with a supercritical one for $x_0 = 15$. The 2 subplots on the left show different time snapshots of the evolution of the two-dimensional contour plot of the wavefunction square modulus for $x_0 = 10$. The 4 subplots on the right show the corresponding snapshots for $x_0 = 15$ in the unstable case, leading to the emission of a vortex pair.

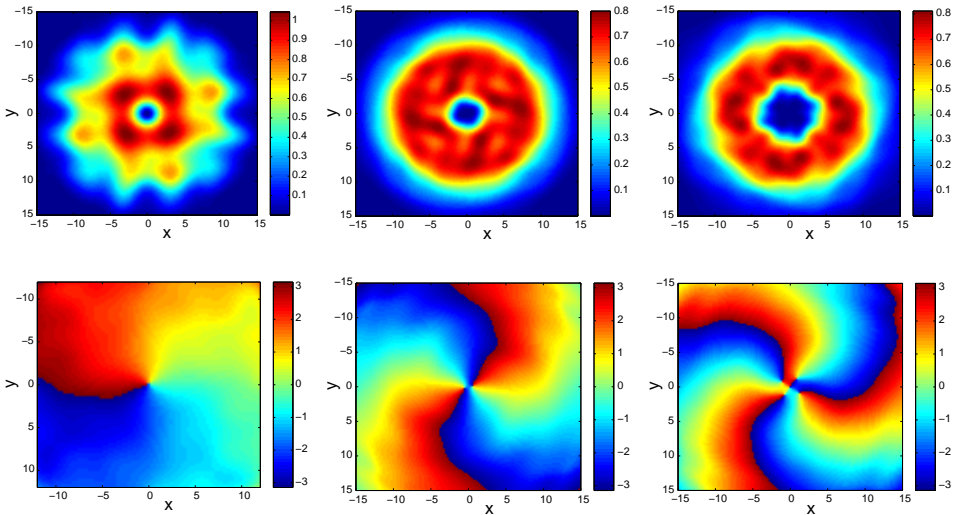


Fig. 2. Phase imprinting of vortices inside the combined magnetic and optical trap (left: for vortices of charge $S = 1$) and solely in the magnetic trap (middle and right: for $S = 2$ and $S = 3$, respectively). The top and bottom row depict, respectively, the atomic density and phase. Left to right: vortices of increasing topological charge of one, two and three. In all cases, a radial magnetic trap frequency of $\Omega = 0.1$ has been used, while for the left panel the optical has been chosen with $\lambda_x = \lambda_y = 4\pi$, and $\phi_x = \phi_y = 0$, while $V_0 = 0.25$.

(through an appropriate “phase mask”) of a phase difference of 2π around a contour can generate vortex structures (which carry topological charge). In fact, this method was proposed as a means of preparing vortex states in 2D BECs in Ref. 56 and was

subsequently used in the laboratory in the experiments of Ref. 24. Some of the advantages that this technique has over the previous ones are that:

1. It is very robust in the presence of even strong perturbations (i.e. it works equally well in the cases of combined potentials such as magnetic and optical ones); see left panels in Fig. 2.
2. It can be straightforwardly generalized to produce vortices of higher charge. These vortices may also be observed (for appropriate parameter values) to be dynamically stable for very long times and hence should, in principle, be experimentally observable; see middle and right panels in Fig. 2.

3.2. Dynamical stability

3.2.1. Continuum models

Let us now address the question of stability of vortices trapped in a combined MT and OL as described in Ref. 57. Consider a quasi-two-dimensional¹² condensate where a single vortex has been generated at the center of the combined potential

$$V_{\text{ext}}(x, y) = V_{\text{MT}}(x, y) + V_{\text{OL}}(x, y), \tag{9}$$

where the contributions to the MT and OL, are given by the 2D equivalents of (2) and (3), respectively. As mentioned in the previous section, the effective 2D GP equation [cf. Eq. (6)] applies to situations where the condensate has a nearly planar (“pancake”) shape (see for example Ref. 58 and references therein). Accordingly, vortex states considered below are not subject to 3D instabilities (corrugation of the vortex axis³⁹) as the transverse dimension is effectively suppressed.

The stability of the vortex at the center of the trap can be qualitatively understood in terms of an effective potential obtained by means of a variational approximation.⁵⁹ As in Ref. 60, we use the following ansatz to approximate the position $r_0(t) = (x_0(t), y_0(t))$ of vortex near the trap center

$$\Psi(x, y, t) = B(t) \|r_0(t)\| \exp[-\|r_0(t)\|^2/b(t)] e^{i\varphi_0(t)}, \tag{10}$$

where $\varphi_0(t) \equiv \tan^{-1}[(y - y_0(t))/(x - x_0(t))]$ denotes the 2-norm of the vector r_0 . Similarly to the calculations in Refs. 61 and 62, or upon employing the conservation of norm, it is straightforward to show that, to leading order, $B(t) = B(0)$ and $b(t) = b(0)$ are approximately constant. Then, assuming the same detuning and periodicity in all directions (i.e. $\phi_x = \phi_y = \phi$ and $\lambda_x = \lambda_y = \lambda$), the substitution of the ansatz (10) into the Lagrangian form of the GP equation (6) leads to a quasiparticle description of the vortex center through the Newton-type equations of motion

$$\ddot{x}_0 = -\frac{dV_{\text{eff}}(x_0, y_0)}{dx_0} \quad \text{and} \quad \ddot{y}_0 = -\frac{dV_{\text{eff}}(x_0, y_0)}{dy_0}, \tag{11}$$

where the effective potential is given by

$$V_{\text{eff}}(x, y) = Q(\phi) \left[\cos\left(\frac{4\pi x}{\lambda}\right) + \cos\left(\frac{4\pi y}{\lambda}\right) \right] + \frac{1}{4}\Omega^2 (x^2 + y^2), \tag{12}$$

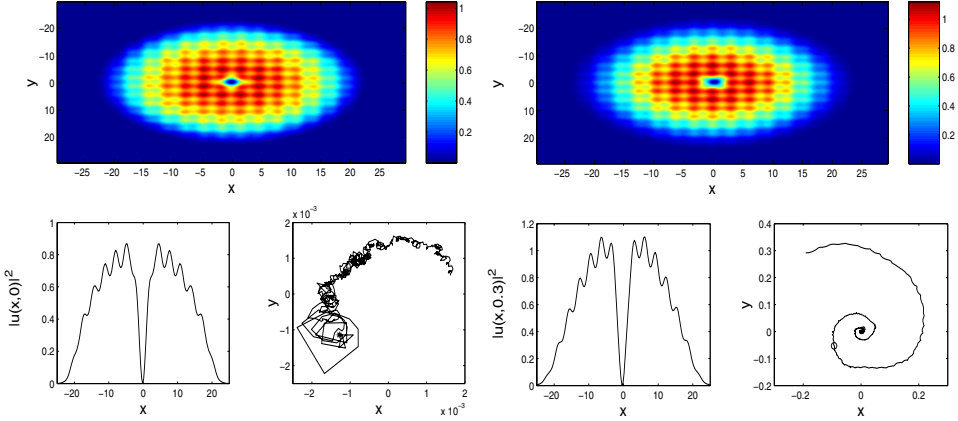


Fig. 3. Vortex stability inside a combined magnetic and optical trap. The MT and OL parameters are $\omega_x^2 = \omega_y^2 = 0.002$, $V_0 = 0.5$ and $\lambda = \lambda_x = \lambda_y = 2\pi$. Left: the vortex is stable at the bottom of a cosinusoidal OL [$\phi = 0$ in Eq. (3)]. The top panel shows the contour plot of the density at $t = 100$ (138 ms). The bottom left panel is a cut of the same density profile along $x = 0$, while the bottom right one shows the motion of the vortex center for $0 \leq t \leq 100$, the initial position being marked by a star. Notice the scale (10^{-3} , or 1 nm in physical units) of very weak motion of the vortex, which thus stays practically immobile at the origin. Right: same as left panels but with a sinusoidal OL [$\phi = \pi/2$] and for a larger time of $t = 250$ (346 ms). The bottom right panel depicts the motion of the vortex center for $0 \leq t \leq 250$ [positions of the vortex center at $t = 100$ (138 ms) and $t = 200$ (276 ms), respectively, are indicated by the star and circle].

and $Q(\phi)$ is given by a rather cumbersome expression. In our case of interest we will only need the following values

$$Q(0) = \frac{V_0}{4} \left(\frac{2b\pi^2}{\lambda^2} - 1 \right) \exp\left(\frac{-2b\pi^2}{\lambda^2}\right), \quad \text{and} \quad Q\left(\frac{\pi}{2}\right) = -Q(0). \quad (13)$$

Equations (11) and (12) indicate that the coordinates of the vortex center are prescribed by two uncoupled nonlinear oscillators (see also Ref. 63 for a similar result in the context of optics). The above, generalizes the well known result⁶⁴ that the center of a dark soliton (the 1D “sibling” of the vortex) behaves like a Newtonian particle in the presence of the external potential (see relevant work for dark matter-wave solitons in optical lattices in Ref. 65). Figure 3 depicts the vortex stability for the two detuning cases in (13). For $\lambda = 2\pi$, $V_0 = 0.5 > 0$ and $b = 1$ (by fitting ansatz to numerical solution), we have that $Q(\phi = 0) = -V_0/8 < 0$ and $Q(\phi = \pi/2) = -Q(0) = V_0/8 > 0$. Therefore, a cosinusoidal OL ($\phi = 0$) produces a stable vortex (see left panels of Fig. 3) while a sinusoidal OL ($\phi = \pi/2$) induces an instability (see right panels of Fig. 3). Note that, recently, relevant results have been obtained using different approaches.⁶⁶

It is worth mentioning that the variational approach outlined above, although capable of capturing the stability of the vortex at the center of the trap, fails to reproduce the correct dynamics. More specifically, as shown in Fig. 3, the vortex center follows an outward spiraling motion. This spiral motion is the combination of the unstable behavior captured by the Hamiltonian dynamics of Eqs. (11) and (12)

together with the well known precession of vortices inside the MT.⁶⁷ The precession, not captured by our approximation, predicts that, close to the trap center, a vortex rotates with an angular frequency given by⁶⁷

$$\omega_{\text{prec}} = \frac{-3\omega_x\omega_y}{4\mu} \ln\left(\frac{R_{\text{BEC}}}{\xi}\right), \tag{14}$$

where μ is the chemical potential, R_{BEC} is the mean transverse dimension of the condensate and ξ is the width of the vortex core, which, in fact, is the same as the healing length of the condensate.⁷

3.2.2. Discrete models

An interesting situation arises for strong optical lattices ($V_0 \gg \mu$) where the condensate is effectively transformed into a collection of “droplets” (in each lattice well) that can be described by the spatially discrete analogue of the NLS.^{15,17,18,21,68} In this case, it is possible to describe the evolution of the condensate wavefunction by the discrete nonlinear Schrödinger equation (DNLS) as can be seen through a Wannier function decomposition.^{69,70} In nondimensional units, the DNLS reads

$$i\frac{d}{dt}\phi_\eta + C\Delta_2^{(d)}\phi_\eta + |\phi_\eta|^2\phi_\eta = 0, \tag{15}$$

where ϕ_η is the condensate wavefunction localized at the OL trough with coordinates $\eta = (m, n)$ and $\eta = (l, m, n)$, for the 2D and 3D cases respectively, C is the coupling constant, and $\Delta_2^{(d)}$ stands for the discrete Laplacian in d dimensions:

$$\Delta_2^{(2)}\phi_{m,n} = \phi_{m+1,n} + \phi_{m,n+1} + \phi_{m,n-1} + \phi_{m-1,n} - 4\phi_{m,n}$$

and

$$\begin{aligned} \Delta_2^{(3)}\phi_{l,m,n} &= \phi_{l+1,m,n} + \phi_{l,m+1,n} + \phi_{l,m,n+1} + \phi_{l-1,m,n} \\ &\quad + \phi_{l,m-1,n-1} + \phi_{l,m,n-1} - 6\phi_{l,m,n}. \end{aligned}$$

In Refs. 71, 72 and 73 stationary solutions of (15) are sought by considering $\phi_\eta = \exp(-i\mu_0 t)u_\eta$, where μ_0 is the dimensionless chemical potential of the condensate, that yields to the time-independent equation:

$$-\mu_0 u_\eta = C\Delta_2^{(d)}u_\eta + |u_\eta|^2 u_\eta, \tag{16}$$

where $|u_\eta|^2$ is proportional to the atomic density at the η th trough. Since Eq. (16) has a scale invariance, μ can be fixed arbitrarily. As in Refs. 71, 72 and 73, by using an appropriate initial discrete vortex ansatz, it is possible to find numerical solutions to Eq. (16). Then, by applying continuation-type methods, together with linear stability computations, the branches of existence and stability for discrete vortices of different charges in two- ($d = 2$) and three-dimensional ($d = 3$) settings can be obtained.

The stability results presented in Refs. 71 and 73, for vortices of charge S (e.g. for dimensionless chemical potential $\mu_0 = -4$), can be summarized in the following stability table:

d	$S = 0$	$S = 1$	$S = 3$	$S = 2$
2	$C \lesssim C_{\text{cr}}^{(2,0)} \approx 4$	$C \lesssim C_{\text{cr}}^{(2,1)} \approx 1.6$	$C \lesssim C_{\text{cr}}^{(2,3)} \approx 0.398$	U

where the approximate region for stability is indicated (the letter “U” denotes unstable for all values of C). As indicated, no stable vortices with $S = 2$ were obtained.⁷⁴ Nonetheless, Eq. (16) admits *real* stationary solutions — generated by the real part of the corresponding genuine vortex (which is complex) — that are stable for sufficiently weak coupling. These real solutions, the so-called quasi-vortices, correspond to quadrupoles ($S = 2$) and octupoles ($S = 4$).^{71,73} Similar results were found also for the three-dimensional case in Ref. 72. In Fig. 4 we depict a few examples of discrete vortices for different vorticities in two and three dimensions.

It is important to mention that the discreteness is responsible for inducing the stability of vortices in three-dimensional settings that otherwise (in the continuum model) are strongly unstable. A natural question that arises is the fate of unstable solutions. For example, we have observed that, in two dimensions, a vortex with $S = 3$ and $C = 0.618 > C_{\text{cr}}^{(2,3)}$ may decay into a configuration consisting of a combination of a stable soliton ($S = 0$) and a stable $S = 1$ vortex (here $C < C_{\text{cr}}^{(2,0)}$ and $C < C_{\text{cr}}^{(2,1)}$). On the other hand, we have observed a striking effect where, in three dimensions, an unstable $S = 2$ vortex decays into a *stable* $S = 3$ vortex (for $C = 0.01 < C_{\text{cr}}^{(3,3)}$), thereby increasing the total topological charge instead of decaying to a combination of lower order ($S = 0, 1$) vortices. It should be noted that this change of vorticity is possible in the discrete lattice model, in which the angular momentum is not a dynamical invariant. Another noteworthy vortex solution also found in Ref. 72 consists of a complex of two mutually orthogonal $S = 1$ vortices (one in each component) in the discrete version of a two-component condensate (cf. Sec. 4.2).

4. Two Vortices

4.1. One-component BEC: interactions

Up to this point we have dealt with the generation and stability of vortices. Let us now focus on the important issue of vortex–vortex interactions. As is the case also for fluid vortices, two BEC vortices of opposite charge travel parallel to each other at constant speed c , while vortices of same charge rotate at constant angular speed α .^{75,76} From direct numerical integration of Eq. (6) we have been able to characterize the dynamics of interacting vortices in the absence of any trapping potential ($\Omega = 0$). With an appropriate initial phase mask (see Sec. 3.1) we seeded two vortices, with respective vorticities S_1 and S_2 , at a desired distance from each other. Then, we fitted a Padé approximation⁷⁷ to find the vortex centers during

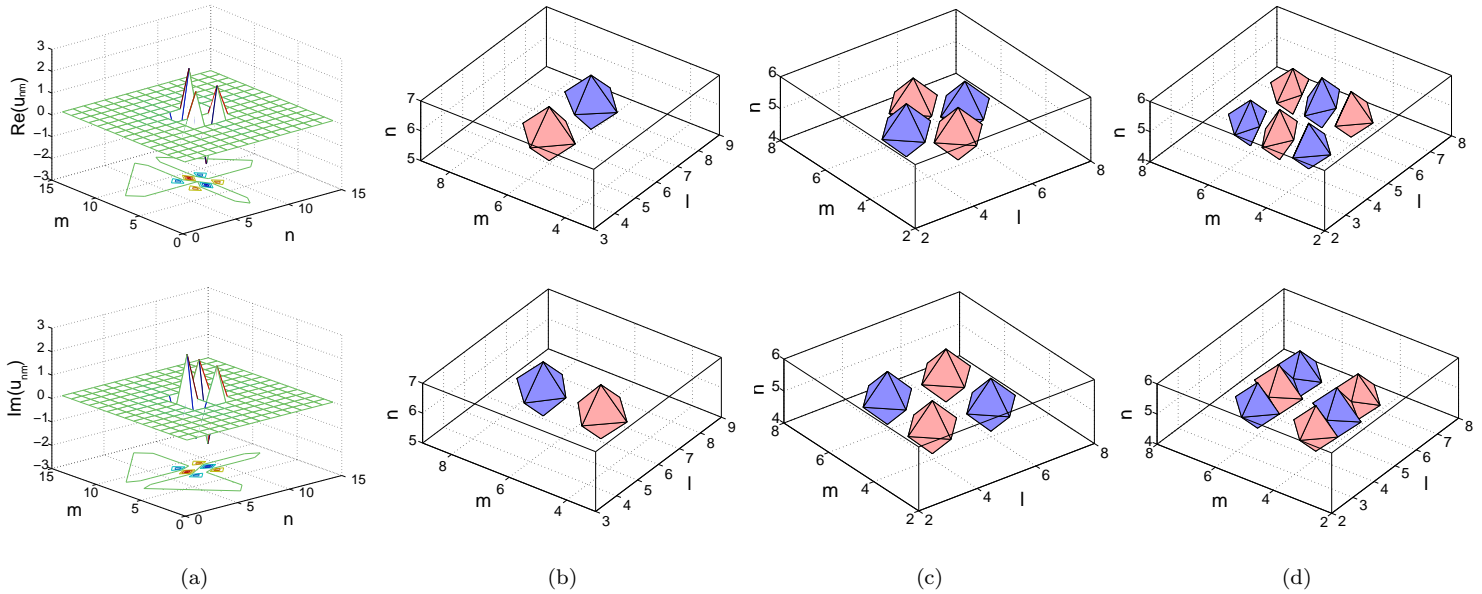


Fig. 4. Vortices in the discrete nonlinear Schrödinger equation in two ($d = 2$) and three ($d = 3$) dimensions. The top (bottom) row depicts the real (imaginary) part of the stationary solution [cf. Eq. (16)] with vorticity S . For $d = 3$ (b, c, d) the plots depict the contour plots for $\text{Re}(u_{l,m,n}) = \pm\text{constant}$ (top row) and $\text{Im}(u_{l,m,n}) = \pm\text{constant}$ (bottom row). The parameters are, from left to right: (a) $d = 2$, $S = 3$, $C = 0.02$ (b) $d = 3$, $S = 1$, $C = 0.7$, constant = 0.5 (c) $d = 3$, $S = 2$, $C = 0.01$, constant = 0.25 and (d) $d = 3$, $S = 3$, $C = 0.01$, constant = 0.25.

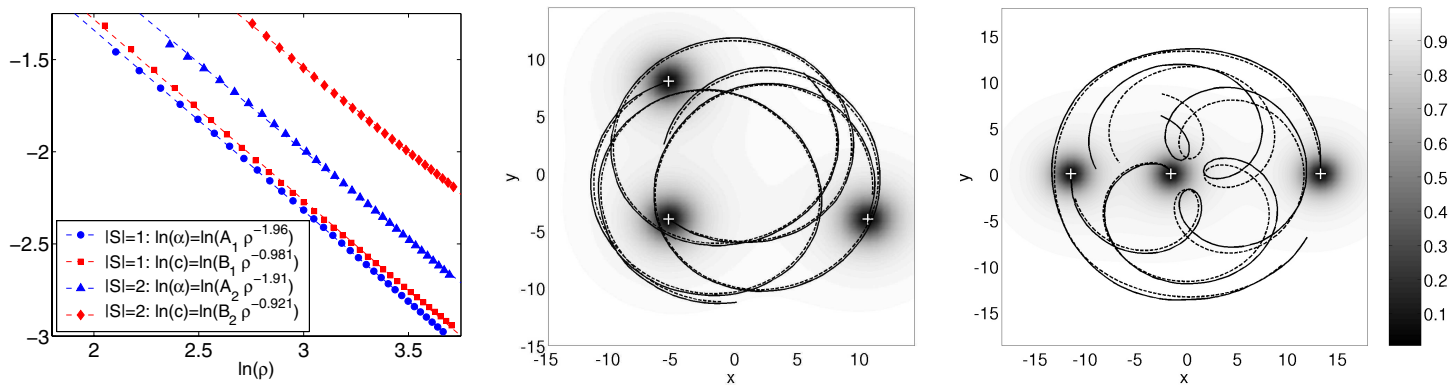


Fig. 5. Left: linear $c(\rho)$ (angular $\alpha(\rho)$) velocity for two vortices of opposite (equal) charge $|S| = |S_1| = |S_2| = 1$ and $|S| = |S_1| = |S_2| = 2$ as a function of their separation distance ρ . Middle and right panels depict two configurations of three interacting vortices of charge $S = 1$. The *solid* and *dashed line* represent the trajectories of their centers from direct numerical integration of (1) and from the quasiparticle approximation of (18), respectively.

evolution, and numerically extracted the linear (angular) velocities for vortices of opposite (equal) charge as a function of their separation distance ρ (see left panel in Fig. 5). We performed our experiments for same and opposite charge vortices with vorticities $|S_1| = |S_2| = 1$ and $|S_1| = |S_2| = 2$. The angular and linear velocities of interacting vortices seem to nicely obey power-laws for a wide range of separations ($10 < \rho < 50$): $c(\rho) \sim \rho^{-1}$ and $\alpha(\rho) \sim \rho^{-2}$ (see left panel of Fig. 5).

The next step to describe the dynamics of interacting vortices consists on identifying an appropriate Lagrangian that gives rise to the correct dynamics. In order to achieve this, it is crucial to note that BEC vortices are known to obey first order, kinematic equations,³⁹ contrary to what is known for the Newtonian (second order) equations describing other types of solitary wave center of mass dynamics.⁵⁹ To circumvent this obstacle, we need to construct an interaction Lagrangian that gives the “correct” vortex dynamics through its Euler–Lagrange equations. Such a Lagrangian for two vortices, with *same* vorticity $S = S_m = S_n$, may be given in the form

$$L_{m,n} \sim \det(\dot{\mathbf{r}}_m, \mathbf{r}_m) + \det(\dot{\mathbf{r}}_n, \mathbf{r}_n) - AS \ln(\rho) \tag{17}$$

where $\mathbf{r}_m = (x_m, y_m)^T$ is the position vector of vortex m and A is a constant. For vortices of opposite charge one needs to multiply the velocities for each vortex by their respective charge. This is equivalent to including the vortex charge in the definition of the Poisson brackets for the vortex interaction Hamiltonian (cf. Ref. 78 and references therein).

Let us explicitly write the equations of motion for same charge vortices. In this case, the pairwise Lagrangian (17) gives rise to the well known equations of motion for two (fluid) point vortices centered at $\mathbf{r}_n = (x_n, y_n)^T$ and $\mathbf{r}_m = (x_m, y_m)^T$:

$$\begin{aligned} \dot{x}_m &= -AS \frac{y_m - y_n}{2\rho^2} \\ \dot{y}_m &= +AS \frac{x_m - x_n}{2\rho^2}, \end{aligned} \tag{18}$$

where $\rho = \sqrt{(x_m - x_n)^2 + (y_m - y_n)^2}$ is inter-vortex distance and $A = A_1 \approx 3.96$ for $S = 1$ and $A = A_2 \approx 7.80$ for $S = 2$ is a constant determined from the numerics (cf. left panel in Fig. 5). As expected we have $2A_1 = 7.92 \approx A_2$, namely, the effects of an $S = 2$ vortex are equivalent to the superposition of the effects of two nearby $S = 1$ vortices. For opposite charge vortices traveling parallel to each other at constant speed c , our numerics predict that $c(\rho) = B\rho^{-1}$ with $B = B_1 \approx 2.15$ and $B = B_2 \approx 4.43$ for singly- ($|S| = 1$) and doubly-charged ($|S| = 2$) vortices respectively. As for same charge vortices, the relationship $2B_1 = 4.30 \approx B_2$ holds approximately.

Approximation (18) treats vortex pairs as quasiparticles with interacting potentials. It is important to mention that this approximation to the dynamics deteriorates when the vortices get too close to each other. Nonetheless, we have checked that the approximation remains valid down to separation distances of the order of

the healing length (i.e. the width of the vortices) for $|S| = 1$ vortices. For $|S| = 2$, the two vortices tend to split into two pairs of $S = 1$ vortices⁷⁹ when the separation distance was decreased below approximatively $\rho = 10$.

In the middle and right panel of Fig. 5 we present two examples with three interacting vortices. The solid line represents the actual orbits obtained from direct numerical integration of Eq. (1), while the dashed line depicts the orbits using the quasiparticle approximation (18). As it can be observed from the figure, the superposition of all the interactions, given by (18), for the three vortices is in good agreement with the full model. It is worth mentioning that the case depicted in the right panel of the figure corresponds to an orbit with an initial condition close to an unstable configuration. This explains the larger discrepancy for this case when compared to the middle panel.

We note in passing that a more general approach towards computing vortex interactions may involve the use of a Lagrange multiplier at the level of the PDE (initialized with two vortices) which maintains the distance between the vortices fixed. Then, the force associated with the relevant multiplier is what is needed to balance the interaction force between the vortices and hence can also be used to infer the interaction potential.

4.2. Two-component BECs: dipole bound states

A very relevant generalization of the class of physical systems that we have discussed so far, and of the solitary waves they can support, concerns the case of coupled multi-component BECs. There has recently been a considerable volume of work relevant to the properties of coupled BECs ranging from the study of ground state solutions^{80,81} to small-amplitude excitations.⁸² Furthermore, the formation of various structures such as domain-walls,^{83–86} bound dark-dark,⁸⁶ dark-bright,⁸⁷ dark-antidark, dark-gray, bright-antidark and bright-gray soliton complexes,⁸⁸ as well as spatially periodic states⁸⁹ was also predicted. On the other hand, experimental results have been reported for mixtures of different spin states of ⁸⁷Rb (see Ref. 90) and mixed condensates.^{91,92} It is relevant to also mention the efforts towards the realization of two-component BECs from different atomic species, such as ⁴¹K–⁸⁷Rb (see Ref. 93) and ⁷Li–¹³³Cs (see Ref. 94).

Typically, the generalized mean-field model for two coupled BECs involves two nonlinearly coupled GP equations. However, in experiments with a radio-frequency (or an electric field) coupling two separate hyperfine states,⁹⁰ the relevant model also involves a linear coupling between the wavefunctions. The governing normalized equations are then of the form:

$$i\psi_{1t} = \left[-\frac{1}{2}\Delta + V + g_{11}|\psi_1|^2 + g_{12}|\psi_2|^2 \right] \psi_1 + \alpha\psi_2, \quad (19)$$

$$i\psi_{2t} = \left[-\frac{1}{2}\Delta + V + g_{12}|\psi_1|^2 + g_{22}|\psi_2|^2 \right] \psi_2 + \alpha\psi_1, \quad (20)$$

where the intra- and interspecies interactions are characterized by the coefficients

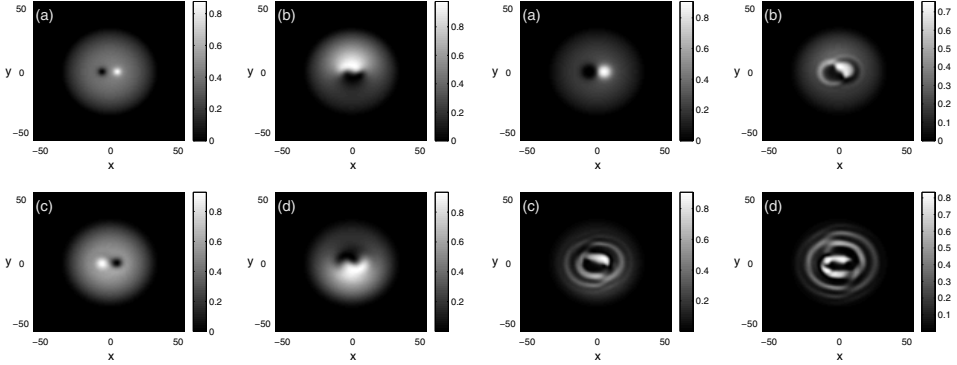


Fig. 6. Left panels: Contour plots of $|\psi_1|^2$ for two coupled vortices, initially placed at $x = \pm 5$, for (a) $t = 0$, (b) $T/4$, (c) $T/2$ and (d) $3T/4$, with $T = \pi/\alpha \approx 15.7$ ($\alpha = 0.2$); $\Omega = 0.045$, $\Delta \equiv g_{11}g_{22} - g_{12}^2 = -9 \times 10^{-4}$ (^{87}Rb). The vortices “interchange locations” (in a structure resembling a spiral wave). Right panels: Same as the left but for $\Delta = -3$ ($g = 1, h = 2$). The configuration breaks up forming spiral patterns.

g_{jj} ($j = 1, 2$) and g_{12} respectively, while α denotes the strength of the radio-frequency (or electric field) coupling. In the recent work of Ref. 95, the special case of $g_{11} = g_{22} = g_{12} \equiv g$ was examined. The latter can be written in a vector form as:

$$i\psi_t - \alpha P\psi = -\frac{1}{2}\Delta\psi + (\psi^\dagger G\psi)\psi + V(\mathbf{x})\psi, \tag{21}$$

where

$$P = \begin{pmatrix} 0 & 1 \\ 1 & 0 \end{pmatrix} \tag{22}$$

and $G = g\mathbf{I}$, with \mathbf{I} being the unit matrix. In that case, as was also previously known in optics,⁹⁶ one can make a unitary transformation:

$$\psi = U(t)\psi_0 = e^{-i\alpha Pt}\psi_0 = \begin{pmatrix} \cos(\alpha t) & -i\sin(\alpha t) \\ -i\sin(\alpha t) & \cos(\alpha t) \end{pmatrix} \psi_0. \tag{23}$$

Then the original set of equations is transformed into:

$$i\psi_{0t} = -\frac{1}{2}\Delta\psi_0 + (\psi_0^\dagger G\psi_0)\psi_0 + V(\mathbf{x})\psi_0, \tag{24}$$

i.e. the linear coupling can be completely eliminated from the equations. Notice that this special case of approximately equal scattering length coefficients is relevant to the experiments performed with two spin states of ^{87}Rb (see Ref. 91), where $g_{11} : g_{12} : g_{22} = 1.03 : 1 : 0.97$.

In the system of nonlinearly coupled GP equations for ψ_0 , one can construct a dipole configuration with a pair of vortex structures, see Fig. 6. This configuration was obtained in the figure, by means of imaginary time integration in the absence of linear coupling, starting with one component having a vortex centered at $(5, 0)$, while the other having a vortex at $(-5, 0)$. After the configuration relaxes to the

stationary vortex pair solution of Eqs. (19) and (20), one can turn on the linear coupling and obtain a spiral rotation between the vortices resembling a spiral wave. While this solution is *exact* for $h \equiv g_{12}/g_{11} = 1$ (assuming $g_{11} = g_{22}$), it also persists for non-unit values of h . In particular, the spiral structure persists for $h < h_c = 1.32$ beyond which the regularity of the Rabi oscillations of matter between the components is destroyed. In this case, the breakup leads to the formation of spiral patterns in the condensate.⁹⁵

5. Vortex Lattices

We now turn to a “thermodynamic limit” level which is also, however, particularly relevant to BEC experiments. Rapid rotation of 2D BECs induces the generation of many vortices^{39,97,98} that typically settle into ordered lattices.^{25–29,99,100} Particularly enticing in this respect are the available pictures of such lattices and their (practically perfect) triangular patterns.¹⁰¹ These are the so-called Abrikosov lattices,¹⁰² that were long ago predicted in the theory of superconductivity (and that are cited as the prediction that earned their discoverer the Nobel prize in Physics in 2003). In the context of type-II superconductors, free energy arguments can be used to demonstrate that the triangular lattice is the most energetically favorable (ground-state) configuration.¹⁰³

It is quite interesting in this context, to study vortex lattices in the framework of Eq. (6) both in the presence of the external magnetic trap (MT), as well as in the one of the optical lattice (OL). Naturally, it is relevant to perform direct simulations of such lattices for different (external potential) parameter values. However, a quite relevant alternative tool in order to study the ground states of such configurations and their structural transitions is the use of molecular dynamics (MD) techniques such as the Parrinello–Rahman (PR) method.¹⁰⁴ In the PR dynamics, not only are the positions of the vortices (viz. particles) evolved in time, but so are the coordinate vectors of the box in which the coherent structures are located. In particular, if the system of coordinates consists of the vectors $\mathbf{a} = (a_x, a_y)$ and $\mathbf{b} = (b_x, b_y)$, then the metric tensor becomes (in 2D) $G = h^T h$, where h is the coordinate transformation matrix with \mathbf{a} , \mathbf{b} as its rows $[(x_m, y_m)^T = h \cdot (\xi_n, \eta_n)^T]$. Then the Lagrangian for the fictitious coupled dynamics of the “particle”-lattice and the MD box reads^{104,105}:

$$\begin{aligned} \mathcal{L} = & \frac{1}{2} \sum_n M(G_{11}\dot{\xi}_n^2 + 2G_{12}\dot{\xi}_n\dot{\nu}_n + G_{22}\dot{\nu}_n^2) \\ & + \frac{1}{2}W(\dot{a}_x^2 + \dot{a}_y^2 + \dot{b}_x^2 + \dot{b}_y^2) - \sum_{m,n} V_{mn} \end{aligned} \quad (25)$$

where M, W are the particle and box mass respectively, (ξ_n, ν_n) are the coordinates of the n th particle in the “box frame”, V_{mn} is the interaction potential between quasiparticles m and n , and the summations are over the total number of vortices N_v . Then, one can perform PR-MD by solving the ensuing dynamical equations,^{104,105} to obtain the coordinate system evolution (along with that of

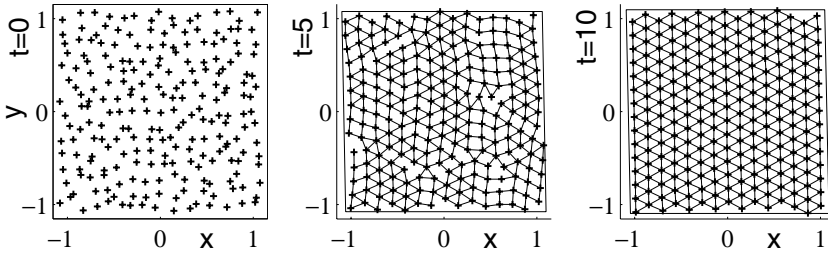


Fig. 7. Typical vortex lattice MD simulation with a random initial pattern of $N_v = 225$ same-charge vortices. After a short transient ($t < 8$), the configuration equilibrates into a triangular lattice ($t = 10$).

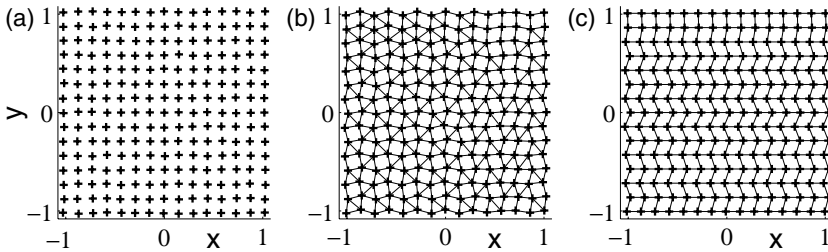


Fig. 8. Molecular dynamics simulations with an initial pattern (a) corresponding to a slightly perturbed square lattice of $N_v = 225$ same-charge vortices. (b) After some transient, the configuration equilibrates to a star pattern. (c) Rhomboidal pattern obtained from a slightly different initial perturbation of (a).

the “particle” positions). More specifically, from (25) one obtains the dynamics for each of the $4N_v + 8$ degrees of freedom, say q_n and \dot{q}_n , via the Euler–Lagrange equations $d/dt(\partial\mathcal{L}/\partial\dot{q}_n) = \partial\mathcal{L}/\partial q_n$. In order to emulate the thermodynamic limit of the system (large number of vortices), the *minimal image convention* can be employed where the box is periodically repeated for all of its 8 neighbors and, for each vortex, the N_v largest contributions, from all the 9 boxes, are taken into account. The results obtained in Ref. 106 indicate that, interacting spiral vortices in a Ginzburg–Landau field-theoretic context¹⁰⁷ (which, in fact, is a dissipative version of the GP equation — see also Ref. 108), typically settle, for sufficiently large number of vortices, to configurations similar to the experimentally observed triangular configuration (see Fig. 7). Note that similar results can be applied to pulses where the topological charge is zero.

In order to specifically apply the PR-MD simulation to a gas of vortices in the BEC model (1), one needs to recast the MD Lagrangian (25) using the realistic vortex-vortex Lagrangian (17).¹⁰⁹ The form of the Lagrangian (25) allows for a direct incorporation of the effects induced by the MT and OL. It is also possible to study the configuration changes in the presence of quadrupolar excitations or other symmetry stresses exerted on the vortex lattice (motivated by the experiments of Refs. 29, 99 and 100). We should note that the external imposition, in the box

containing the vortices, of shear stresses of different symmetry is quite feasible experimentally. It can be implemented through a rotating laser manipulating the boundary of the box (in this case, the periphery of the Thomas–Fermi cloud).¹¹⁰

The PR-MD approach is therefore a powerful tool that can be used to identify the conditions for which the triangular state persists as the ground state configuration (for such conditions, see for example Ref. 111). It can also be used to obtain the structural transition points (obtained through direct simulations, e.g. in the presence of the optical lattice in Ref. 112) to other states such as rhomboidal or star-like patterns (see for example Fig. 8). The approach consists of analyzing the dynamically obtained PR-MD states through stability computations, standard continuation and bifurcation theory tools to explore the structural phase transitions and to obtain the instability eigenvectors that lead to phase transformations. An alternative dynamical scenario, very relevant to recent experimental settings, involves the annihilation of a central chunk of vortex lattice matter, through a localized laser heating,¹⁰⁰ that results in the remaining vortex lattice exhibiting oscillatory modes, known as Tkachenko oscillations. Such modes may also be identified¹⁰⁹ as limit-cycle, time-periodic solutions of the PR-MD numerical procedure.

6. Summary and Outlook

While there is a large volume of work on the waves of topological charge in Bose–Einstein condensates (a large fraction of which is summarized in Ref. 39, as well as in the present brief review), there are still numerous open problems regarding the vortex state that this experimentally and theoretically tractable context may allow us to explore.

Clearly, a prominent position among such open problems (in the context of isolated vortices) is the question of a mathematical understanding of the detailed dynamical stability picture of vortices of various topological charges ($S \geq 1$) in the presence of the combined magnetic and optical trappings. A first step in that direction is offered by the work of Ref. 113; however there are still many open questions concerning the effect of the trapping potentials.

Another subject that apparently has received very little attention and whose theoretical understanding is still to a large extent incomplete (in the context of few vortices) is the behavior of vortex dipoles. Such configurations have been now obtained for two-component BECs in the work of Refs. 95 and 114, however topics such as the interaction of such dipoles and the ensuing dynamics are still unexplored. From the mathematical point of view, a first attempt at obtaining reduced equations that adequately describe dipole dynamics has been given in Ref. 115. The applicability of such an approach in the context of BECs would be of particular interest.

There are also numerous interesting open questions regarding vortex lattices. The dynamical imposition/time dependence of external potentials in conjunction with possible interaction between multiple condensate components may produce

interesting effects of frustration that may induce structural phase transitions such as the ones discussed in Ref. 112 (e.g. a reshaping from a triangular lattice to a square one; see for example Ref. 116). The PR-MD setup is straightforwardly amenable to the inclusion of such external effects. By properly incorporating a 2D OL, we expect to induce a locally attractive (or locally repulsive) energy landscape for each vortex at any required location. This should enable us to *engineer* a rich variety of “target” lattice configurations —provided that their energy is not far from a local minimum. Applications of these (as well as statistical mechanics) techniques to understand the ground state of vortex lattices under external perturbations or multi-component interactions are bound to provide interesting conclusions for the non-equilibrium thermodynamics of such multi-vortex patterns. Notice that some of these tasks (such as identifying stationary vortex lattice states and computing the corresponding eigenvalues of linearization around them) can be performed by methods that have been developed in matrix-free numerical linear algebra.¹¹⁷ This can be done by using appropriately initialized short bursts of time evolution simulations instead of the very expensive large Jacobian eigenvalue computations.

These are only some among the many questions/topics that are now starting to be addressed (for instance, one can ask the same questions at finite temperature and try to understand the interaction of the vortex condensate with the gas in that case). We hope that this intriguing journey still hides, as Cavafy says in his *Ithaca*, a lot of “ports seen for the first time . . .”

Acknowledgments

It is a real pleasure to acknowledge the invaluable contribution of our collaborators in many of the topics discussed here: Egor Alfimov, Alan Bishop, Fotis Diakonou, Todd Kapitula, Yuri Kivshar, Volodya Konotop, Boris Malomed, Dimitri Maroudas, Alex Nicolin, Hector Nistazakis, Dmitry Pelinovsky, Mason Porter, Nick Proukakis, Mario Salerno, Peter Schmelcher, Augusto Smerzi, Giorgos Theocharis and Andrea Trombettoni are greatly thanked. We would also like to acknowledge numerous useful discussions with Peter Engels and David Hall. PGK is grateful to the Eppley Foundation for Research, the NSF-DMS-0204585 and the NSF-CAREER program for financial support. RCG acknowledges the support of an SDSU Foundation Grant-In-Aid. DJF acknowledges the support of the Special Research Account of University of Athens. IGK acknowledges the support of an NSF-ITR grant.

Note Added in Proof

Another recent work that tackles the effects of external potentials (such as an optical lattice) on a vortex lattice is that of Ref. 118. Pinning type phenomena are observed as a function of the system parameters and the relevant phase diagrams are obtained.

References

1. S. N. Bose, *Z. Phys.* **26** (1924) 178.
2. A. Einstein, *Sitzber. Kgl. Preuss. Akad. Wiss.* **261** (1924).
3. A. Einstein, *Sitzber. Kgl. Preuss. Akad. Wiss.* **3** (1925).
4. M. H. J. Anderson, J. R. Ensher, M. R. Matthews and C. E. Wieman, *Science* **269** (1995) 198.
5. K. B. Davis, M.-O. Mewes, M. R. Andrews, N. J. van Druten, D. S. Durfee, D. M. Kurn and W. Ketterle, *Phys. Rev. Lett.* **75** (1995) 3969.
6. C. C. Bradley, C. A. Sackett, J. J. Tollett and R. G. Hulet, *Phys. Rev. Lett.* **75** (1995) 1687.
7. F. Dalfovo, S. Giorgini, L. P. Pitaevskii and S. Stringari, *Rev. Mod. Phys.* **71** (1999) 463.
8. E. P. Gross, *J. Math. Phys.* **4** (1963) 195.
9. L. P. Pitaevskii, *J. Exp. Theo. Phys.* **13** (1961) 451.
10. C. Sulem and P. L. Sulem, *The Nonlinear Schrödinger Equation* (Springer-Verlag, New York, 1999).
11. S. Inouye, M. R. Andrews, J. Stenger, H. J. Miesner, D. M. Stamper-Kurn and W. Ketterle, *Nature* **392** (1998) 151.
12. S. Burger, F. S. Cataliotti, C. Fort, P. Maddaloni, F. Minardi and M. Inguscio, *Europhys. Lett.* **57** (2002) 1.
13. A. Görlitz, J. M. Vogels, A. E. Leanhardt, C. Raman, T. L. Gustavson, J. R. Abo-Shaer, A. P. Chikkatur, S. Gupta, S. Inouye, T. Rosenband and W. Ketterle, *Phys. Rev. Lett.* **87** (2001) 130402; S. Burger, F. S. Cataliotti, C. Fort, F. Minardi, M. Inguscio, M. L. Chiofalo and M. P. Tosi, *Phys. Rev. Lett.* **86** (2001) 4447.
14. B. P. Anderson and M. A. Kasevich, *Science* **282** (1998) 1686.
15. F. S. Cataliotti, S. Burger, C. Fort, P. Maddaloni, F. Minardi, A. Trombettoni, A. Smerzi and M. Inguscio, *Science* **293** (2001) 843.
16. J. H. Denschlag, J. E. Simsarian, H. Haffner, C. McKenzie, A. Browaeys, D. Cho, K. Helmerson, S. L. Rolston and W. D. Phillips, *J. Phys.* **B35** (2002) 3095.
17. A. Trombettoni and A. Smerzi, *Phys. Rev. Lett.* **86** (2001) 2353.
18. F. K. Abdullaev, B. B. Baizakov, S. A. Darmanyan, V. V. Konotop and M. Salerno, *Phys. Rev.* **A64** (2001) 043606.
19. O. Morsch and E. Arimondo, Ultracold atomics and Bose–Einstein condensates in optical lattices, in *Dynamics and Thermodynamics of Systems with Long-Range Interactions*, T. Dauxois, S. Ruffo, E. Arimondo and M. Wilkens (eds.) (Springer, Berlin, 2002), pp. 312–331.
20. See e.g. <http://www.mpg.de/~haensch/bec/gallery/>
21. M. Greiner, O. Mandel, T. Esslinger, T. W. Hansch and I. Bloch, *Nature (London)* **415** (2002) 39.
22. M. Kasevich and A. Tuchman (private communication).
23. F. S. Cataliotti, L. Fallani, F. Ferlino, C. Fort, P. Maddaloni and M. Inguscio, *New J. Phys.* **5** (2003) 71.
24. M. R. Matthews, B. P. Anderson, P. C. Haljan, D. S. Hall, C. E. Wieman and E. A. Cornell, *Phys. Rev. Lett.* **83** (1999) 2498.
25. K. W. Madison, F. Chevy, W. Wohlleben and J. Dalibard, *Phys. Rev. Lett.* **84** (1999) 806.
26. S. Inouye, S. Gupta, T. Rosenband, A. P. Chikkatur, A. Görlitz, T. L. Gustavson, A. E. Leanhardt, D. E. Pritchard and W. Ketterle, *Phys. Rev. Lett.* **87** (2001) 080402.
27. J. R. Abo-Shaer, C. Raman, J. M. Vogels and W. Ketterle, *Science* **292** (2001) 476.
28. J. R. Abo-Shaer, C. Raman and W. Ketterle, *Phys. Rev. Lett.* **88** (2002) 070409.

29. P. Engels, I. Coddington, P. C. Haljan and E. A. Cornell, *Phys. Rev. Lett.* **89** (2002) 100403.
30. J. Denschlag, J. E. Simsarian, D. L. Feder, C. W. Clark, L. A. Collins, J. Cubizolles, L. Deng, E. W. Hagley, K. Helmerson, W. P. Reinhardt, S. L. Rolston, B. I. Schneider and W. D. Phillips, *Science* **287** (2000) 97.
31. S. Burger, K. Bongs, S. Dettmer, W. Ertmer, K. Sengstock, A. Sanpera, G. V. Shlyapnikov and M. Lewenstein, *Phys. Rev. Lett.* **83** (2001) 5198.
32. B. P. Anderson, P. C. Haljan, C. A. Regal, D. L. Feder, L. A. Collins, C. W. Clark and E. A. Cornell, *Phys. Rev. Lett.* **86** (2001) 2926.
33. K. E. Strecker, G. B. Partridge, A. G. Truscott and R. G. Hulet, *Nature* **417** (2002) 150.
34. L. Khaykovich, F. Schreck, G. Ferrari, T. Bourdel, J. Cubizolles, L. D. Carr, Y. Castin and C. Salomon, *Science* **296** (2002) 1290.
35. T. Frisch, Y. Pomeau and S. Rica, *Phys. Rev. Lett.* **69** (1992) 1644.
36. T. Winiecki, J. F. McCann and C. S. Adams, *Phys. Rev. Lett.* **82** (1999) 5186.
37. B. Jackson, J. F. McCann and C. S. Adams, *Phys. Rev. Lett.* **80** (1998) 3903.
38. R. J. Donnelly, *Quantized Vortices in He II* (Cambridge University Press, Cambridge 1991).
39. A. L. Fetter and A. A. Svidzinsky, *J. Phys.: Cond. Matt.* **13** (2001) R135.
40. J. J. García-Ripoll and V. M. Pérez-García, *Phys. Rev.* **A63** (2001) 041603(R).
41. Yu. S. Kivshar and B. Luther-Davies, *Phys. Rep.* **298** (1998) 81.
42. Yu. S. Kivshar and D. E. Pelinovsky, *Phys. Rep.* **331** (2000) 117.
43. A. E. Muryshev, H. B. van Linden van den Heuvell and G. V. Shlyapnikov, *Phys. Rev.* **A60** (1999) R2665; P. O. Fedichev, A. E. Muryshev and G. V. Shlyapnikov, *ibid.* **A60** (1999) 3220; D. L. Feder, M. S. Pindzola, L. A. Collins, B. I. Schneider and C. W. Clark, *ibid.* **A62** (2000) 053606; J. Brand and W. P. Reinhardt, *ibid.* **A65** (2002) 043612.
44. N. P. Proukakis, N. G. Parker, D. J. Frantzeskakis and C. S. Adams, *J. Opt. B: Quantum Semiclass. Opt.* **6** (2004) S380.
45. P. G. Kevrekidis, G. Theocharis, D. J. Frantzeskakis and A. Trombettoni, *Phys. Rev.* **A70** (2004) 023602.
46. Yu. S. Kivshar and X. Yang, *Phys. Rev.* **E50** (1994) R40.
47. A. Dreischuh, V. Kamenov and S. Dinev, *Appl. Phys.* **B62** (1996) 139; D. J. Frantzeskakis and B. A. Malomed, *Phys. Lett.* **A264** (1999) 179; H. E. Nistazakis, D. J. Frantzeskakis, B. A. Malomed and P. G. Kevrekidis, *ibid.* **A285** (2001) 157.
48. D. Neshev, A. Dreischuh, V. Kamenov, I. Stefanov, S. Dinev, W. Fliesser and L. Windholz, *Appl. Phys.* **B64** (1997) 429; A. Dreischuh, D. Neshev, G. G. Paulus, F. Grasbon and H. Walther, *Phys. Rev.* **E66** (2002) 066611.
49. G. Theocharis, D. J. Frantzeskakis, P. G. Kevrekidis, B. A. Malomed and Yu. S. Kivshar, *Phys. Rev. Lett.* **90** (2003) 120403.
50. L. D. Carr and C. W. Clark, preprint: cond-mat/0408460 (2004).
51. P. G. Kevrekidis and D. J. Frantzeskakis, *Mod. Phys. Lett.* **B18** (2004) 173.
52. G. Theocharis, P. G. Kevrekidis, D. J. Frantzeskakis, A. R. Bishop and H. E. Nistazakis, Soliton and vortex generation in oscillating Bose–Einstein condensates, preprint.
53. P. G. Saffman, *Vortex Dynamics* (Cambridge University Press, 1992); see also relevant pictures at: <http://www.diam.unige.it/~irro/gallery.html>. Also, see example, Ref. 35 and C. Josserand, Y. Pomeau and S. Rica, *Phys. Rev. Lett.* **75** (1995) 3150 for earlier relevant results in the context of superfluids.

54. E. M. Lifshitz and L. P. Pitaevskii, *Statistical Physics II* (Pergamon Press, Oxford, 1980).
55. B. Wu and Q. Niu, *Phys. Rev.* **A64** (2001) 061603(R).
56. J. E. Williams and M. J. Holland, *Nature* **401** (1999) 568.
57. P. G. Kevrekidis, R. Carretero-González, G. Theocharis, D. J. Frantzeskakis and B. A. Malomed, *J. Phys.* **B36** (2003) 3467.
58. L. Salasnich, A. Parola and L. Reatto, *Phys. Rev.* **A65** (2002) 043614; Y. B. Band, I. Towers and B. A. Malomed, *ibid.* **A67** (2003) 023602.
59. B. A. Malomed, *Prog. Opt.* **43** (2002) 71.
60. J. Tempere and J. T. Devreese, *Physica* **C369** (2002) 28.
61. R. Carretero-González and K. Promislow, *Phys. Rev.* **A66** (2002) 033610.
62. R. Carretero-González and K. Promislow, Breathing behavior of coupled Bose–Einstein condensates: From multi-soliton interactions to homoclinic tangles, preprint available at: <http://www.rohan.sdsu.edu/~rcarrete/publications/>
63. A. N. Yannacopoulos, D. J. Frantzeskakis, C. Polymilis and K. Hizanidis, *Phys. Scripta* **65** (2002) 363.
64. See, example, D. J. Frantzeskakis, G. Theocharis, F. K. Diakonou, P. Schmelcher and Yu. S. Kivshar, *Phys. Rev.* **A66** (2002) 053608 and references therein.
65. G. Theocharis, D. J. Frantzeskakis, P. G. Kevrekidis, R. Carretero-González and B. A. Malomed, Dark soliton dynamics in spatially inhomogeneous media: Application to Bose–Einstein condensates, *Math. Comput. Simulat.*, accepted for publication; G. Theocharis, D. J. Frantzeskakis, R. Carretero-González, P. G. Kevrekidis and B. A. Malomed, Controlling the motion of dark solitons by means of periodic potentials: Application to Bose–Einstein condensates in optical lattices, *Phys. Rev.* **E** (2005), in press; both preprints are available at <http://www.rohan.sdsu.edu/~rcarrete/publications/>
66. N. G. Parker, N. P. Proukakis, C. F. Barenghi and C. S. Adams, *Phys. Rev. Lett.* **92** (2004) 160403; J. W. Reijnders and R. A. Duine, *ibid.* **93** (2004) 060401.
67. A. L. Fetter, *J. Low Temp. Phys.* **113** (1998) 189; A. A. Svidzinsky and A. L. Fetter, *Phys. Rev. Lett.* **84** (2000) 5919; E. Lundh and P. Ao, *Phys. Rev.* **A61** (2000) 063612; J. Tempere and J. T. Devreese, *Solid State Commun.* **113** (2000) 471; D. S. Rokhsar, *Phys. Rev. Lett.* **79** (1997) 2164; S. A. McGree and M. J. Holland, *Phys. Rev.* **A63** (2001) 043608; B. P. Anderson, P. C. Haljan, C. E. Wieman and E. A. Cornell, *Phys. Rev. Lett.* **85** (2000) 2857.
68. A. Smerzi, A. Trombettoni, P. G. Kevrekidis and A. R. Bishop, *Phys. Rev. Lett.* **89** (2002) 170402; G. Kalosakas, K. Ø. Rasmussen and A. R. Bishop, *ibid.* **89** (2002) 030402.
69. G. L. Alfimov, P. G. Kevrekidis, V. V. Konotop and M. Salerno, *Phys. Rev.* **E66** (2002) 046608.
70. V. V. Konotop, G. L. Alfimov, P. G. Kevrekidis and M. Salerno, On the reduction of a nonlinear Schrödinger equation with a periodic potential to a vector lattice, in *Proc. Int. Workshop “Nonlinear Physics: Theory and Experiment. II”*, eds. M. Ablowitz, M. Boiti and F. Pempinelli (World Scientific, Singapore, 2003), pp. 280–286.
71. P. G. Kevrekidis, B. A. Malomed, D. J. Frantzeskakis and R. Carretero-González, Higher-order vortices in nonlinear dynamical lattices, to appear as a book chapter in *Progress in Soliton Research* (Nova Science Publishers, 2004), preprint available at <http://www.rohan.sdsu.edu/~rcarrete/publications/>
72. P. G. Kevrekidis, B. A. Malomed, D. J. Frantzeskakis and R. Carretero-González, *Phys. Rev. Lett.* **93** (2004) 080403.
73. P. G. Kevrekidis, B. A. Malomed, Z. Chen and D. J. Frantzeskakis, Stable higher-

- order vortices and quasi-vortices in the discrete nonlinear Schrödinger equation, *Phys. Rev.* **E70** (2004) 056612.
74. B. A. Malomed and P. G. Kevrekidis, *Phys. Rev.* **E64** (2001) 026601; B. B. Baizakov, B. A. Malomed and M. Salerno, *Europhys. Lett.* **63** (2003) 642.
 75. A. L. Fetter, *Phys. Rev.* **138** (1965) 429.
 76. A. L. Fetter, *Phys. Rev.* **151** (1966) 100.
 77. N. G. Berloff, *J. Phys.* **A37** (2004) 1617.
 78. A. V. Borisov and A. E. Pavlov, *Regul. Chaotic Dyn.* **3** (1998) 28–38.
 79. M. Möttönen, T. Mizushima, T. Isoshima, M. M. Salomaa and K. Machida, *Phys. Rev.* **A68** (2003) 023611.
 80. T.-L. Ho and V. B. Shenoy, *Phys. Rev. Lett.* **77** (1996) 3276; H. Pu and N. P. Bigelow, *ibid.* **80** (1998) 1130.
 81. B. D. Esry *et al.*, *Phys. Rev. Lett.* **78** (1997) 3594.
 82. Th. Busch, J. I. Cirac, V. M. Pérez-García and P. Zoller, *Phys. Rev.* **A56** (1997) 2978; R. Graham and D. Walls, *ibid.* **A57** (1998) 484; H. Pu and N. P. Bigelow, *Phys. Rev. Lett.* **80** (1998) 1134; B. D. Esry and C. H. Greene, *Phys. Rev.* **A57** (1998) 1265.
 83. M. Trippenbach, K. Goral, K. Rzazewski, B. A. Malomed and Y. B. Band, *J. Phys.* **B33** (2000) 4017.
 84. S. Coen and M. Haelterman, *Phys. Rev. Lett.* **87** (2001) 140401.
 85. B. A. Malomed, H. E. Nistazakis, D. J. Frantzeskakis and P. G. Kevrekidis, *Phys. Rev.* **A70**, 043616 (2004).
 86. P. Öhberg and L. Santos, *Phys. Rev. Lett.* **86** (2001) 2918.
 87. Th. Busch and J. R. Anglin, *Phys. Rev. Lett.* **87** (2001) 010401.
 88. P. G. Kevrekidis, H. E. Nistazakis, D. J. Frantzeskakis, B. A. Malomed and R. Carretero-González, *Eur. Phys. J.* **D28** (2004) 181.
 89. B. Deconinck, J. N. Kutz, M. S. Patterson and B. W. Warner, *J. Phys.* **A36** (2003) 5431.
 90. C. J. Myatt, E. A. Burt, R. W. Ghrist, E. A. Cornell and C. E. Wieman, *Phys. Rev. Lett.* **78** (1997) 586.
 91. D. S. Hall, M. R. Matthews, J. R. Ensher, C. E. Wieman and E. A. Cornell, *Phys. Rev. Lett.* **81** (1998) 1539; M. R. Matthews, D. S. Hall, D. S. Jin, J. R. Ensher, C. E. Wieman and E. A. Cornell, *Phys. Rev. Lett.* **81** (1998) 243.
 92. D. M. Stamper-Kurn, M. R. Andrews, A. P. Chikkatur, S. Inouye, H.-J. Miesner, J. Stenger and W. Ketterle, *Phys. Rev. Lett.* **80** (1998) 2027.
 93. G. Modugno, G. Ferrari, G. Roati, R. J. Brecha, A. Simoni and M. Inguscio, *Science* **294** (2001) 1320.
 94. M. Mudrich, S. Kraft, K. Singer, R. Grimm, A. Mosk and M. Weidemüller, *Phys. Rev. Lett.* **88** (2002) 253001.
 95. B. Deconinck, P. G. Kevrekidis, H. E. Nistazakis and D. J. Frantzeskakis, *Phys. Rev.* **A70** (2004) 063605.
 96. M. J. Potasek, *J. Opt. Soc. Am.* **B10** (1993) 941.
 97. H. Aref, P. K. Newton, M. A. Stremler, T. Tokieda and D. L. Vainchtein, Vortex crystals, preprint: TAM report 1008 (2002), available at http://www.tam.uiuc.edu/publications/tam_reports/
 98. D. A. Butts and D. S. Rokhsar, *Nature* **397** (1999) 327.
 99. P. Engels, I. Coddington, P. C. Haljan, V. Schweikhard and E. A. Cornell, *Phys. Rev. Lett.* **90** (2003) 170405.
 100. I. Coddington, P. Engels, V. Schweikhard and E. A. Cornell, *Phys. Rev. Lett.* **91** (2003) 100402.
 101. http://cua.mit.edu/ketterle_group/Projects_2001/Vortex_lattice/Vortex.htm

102. A. A. Abrikosov, *Sov. Phys. JETP* **5** (1957) 1174.
103. V. K. Tkachenko, *Sov. Phys. JETP* **22** (1966) 1282.
104. M. Parrinello and A. Rahman, *Phys. Rev. Lett.* **45** (1980) 1196.
105. M. Parrinello and A. Rahman, *J. Appl. Phys.* **52** (1981) 7182.
106. R. Carretero-González, P. G. Kevrekidis, I. G. Kevrekidis, D. Maroudas, G. Theoharis and D. J. Frantzeskakis, Rahman-Parrinello molecular dynamics for vortex lattices, preprint (2004); available at <http://www.rohan.sdsu.edu/~rcarretero/publications/>
107. I. S. Aranson, L. Kramer and A. Weber, *Physica* **D53** (1991) 376.
108. S. Choi, S. A. Morgan and K. Burnett, *Phys. Rev.* **A57** (1998) 4057.
109. The molecular dynamics approach using realistic vortex interactions is currently work in progress and will be published soon. MPEG movie animations can be found at <http://www.rohan.sdsu.edu/~rcarretero> [Research] [Movies] [Mol. Dyn.]
110. P. Engels, personal communication,
111. N. R. Cooper and S. Komineas, preprint: cond-mat/0404112.
112. H. Pu, L. O. Baksmaty, S. Yi and N. P. Bigelow, preprint: cond-mat/0404750.
113. R. L. Pego and H. Warchall, *J. Nonlinear Sci.* **12** (2002) 347.
114. K. Kasamatsu, M. Tsubota and M. Ueda, preprint: cond-mat/0406150 (2004).
115. P. K. Newton, The dipole interaction, *Disc. Cont. Dyn. Syst.* **B7** (2005) in press.
116. V. Schweikhard, I. Coddington, P. Engels, S. Tund and E. A. Cornell, *Phys. Rev. Lett.* **93** (2004) 210403.
117. C. T. Kelley, *Iterative Methods for Linear and Nonlinear Equations*, Frontiers in Applied Mathematics, Vol. 16 (SIAM, Philadelphia, 1995); see also: C. I. Siettos, C. C. Pantelides and I. G. Kevrekidis, *Ind. Eng. Chem.* **42** (2003) 6919.
118. J. W. Reijnders and R. A. Duine, *Phys. Rev. Lett.* **93** (2004) 060401.